Study of Thermal Dynamics of Defatted Bovine Serum Albumin in D_2O Solution by Fourier Transform Infrared Spectra and Evolving Factor Analysis

BO YUAN,* KOICHI MURAYAMA, and HUIMING YAN

State Key Laboratory of Modern Optical Instrumentation, CNERC for Optical Instrument, Zhejiang University, Hangzhou 310027, China (B.Y., H.Y.); and Department of Biochemistry and Biophysics, Gifu University School of Medicine, Gifu 500-8705, Japan (K.M.)

Fourier transform infrared (FT-IR) spectra have been measured for defatted bovine serum albumin (BSA) in D_2O with a concentration of 2.0 wt % over a temperature range of 26–90 °C and the corresponding difference spectra have been calculated by subtracting the contribution of D_2O at the same temperature. Evolving factor analysis (EFA) by selecting two factors and three factors has been employed to analyze the temperature-dependent difference IR spectra in the 1700–1600 cm^{-1} spectral region of the defatted BSA in D_2O solution. Three-factor EFA has been employed to determine the distinction of the three protein species involved in the process of temperature elevation: native, transitional, and denatured protein. The temperature profiles obtained from three-factor EFA indicate that heat-induced conformational change in the secondary structures of defatted BSA in D_2O undergoes two two-state transitions, a drastic transition and a slight transition, which occur in the temperature ranges of 68–82 °C and 56–76 °C, respectively.

Index Headings: **Bovine serum albumin; BSA; Infrared spectroscopy; Thermal dynamics; Evolving factor analysis; EFA.**

INTRODUCTION

Fourier transform infrared (FT-IR) spectroscopy has been employed in the studies of protein in solution for many years because it is powerful not only for the investigation of the secondary structure of proteins but also for analysis of their dynamics.[1–6] In the IR region, the frequencies of amide vibrations, especially amide I vibrations, are very sensitive to the secondary structure elements of proteins.[7–16] However, the assignment to various secondary structures of proteins in the broad amide I region is not straightforward. Thus, second derivatives, Fourier self-deconvolution (FSD), and curve fitting are usually used to deconvolute the amide I band.[7–16] Recently, two-dimensional (2D) correlation spectroscopy has also been proved to be a powerful technique to resolve the amide I band and investigate its kinetics.[17–25]

Along with the above-mentioned methods, chemometrics are also useful in the investigation of IR spectra of protein in solution.[26–32] Originally introduced by Gampp et al.[33] and successfully improved by Maeder,[34] evolving factor analysis (EFA) is a self-modeling curve resolution (SMCR) technique useful for deconvolving complex series of spectroscopic and sample profiles in multivariate data series. This method has successfully been applied to resolve different problems of chemistry, such as resolution of liquid chromatographic peaks, speciation of metal complexes during titrations, analysis of electron spin resonance, and so on.[35–40] As for the field of spectral analysis, this technique has also been employed for the analysis of ultraviolet–visible (UV-Vis), fluorescence, IR, and Raman spectra.[27,41–46] Navea et al.[45] used combined near-infrared (NIR) and mid-infrared (MIR) spectroscopies and multivariate curve resolution (MCR) to study the temperature-dependent evolution of β-lactoglobulin and have distinguished three pure conformations involved in the process in the working thermal range: native, R-type, and molten globule. In our previous research,[44] EFA has also been successfully used to investigate the temperature-dependent NIR spectra of bovine serum albumin (BSA) in aqueous solution. Window factor analysis (WFA),[47–49] proposed by Malinowski et al., is an alternative SMCR method useful for obtaining profiles in the evolutionary process and has been extensively used in various chemical problems as well as EFA. However, we focus only on the potential of EFA in exploring the thermal denaturation process of protein in solution in this paper, and the potential of WFA will be studied in detail in our further work. The purpose of the present study is to analyze the temperature-dependent IR spectra of defatted BSA in D_2O by EFA. EFA was used to isolate the information in the process of temperature-dependent structural changes in defatted BSA in D_2O solution. We have aimed at revealing the potential of EFA in exploring the variations and thermal dynamics of the secondary structures of proteins in solutions.

Bovine serum albumin is a midsize protein with a molecular weight of approximately 66 500 Da.[50] It has a cigar-shaped form of an ellipsoid of revolution in solution and the ellipsoidal axes of 41.6 × 140.9 Å were estimated by means of birefringence in an electrical field.[50] The heat-induced denaturation of BSA has been investigated extensively not only by thermal analysis techniques[51–53] but also by spectroscopic methods.[23,44,54–56] Most of the studies on the thermal denaturation of protein indicated that heat-induced variation in the secondary structures is a two-state transition. Recently, Michnick[53] investigated the thermal stability of BSA by differential scanning calorimetry (DSC). He found that thermal dynamics of fatty acid containing BSA and defatted BSA in aqueous solution are essentially different. Variations of fatty-acid-containing BSA only occur near 69 °C, while those of defatted BSA occur in two temperature ranges: near 56 °C and 69 °C. But some aspects of the temperature-dependent variations of BSA in solution still remain unexplained.

The present study gives researchers an insight into the secondary structure changes taking place in the heat-induced unfolding process of defatted BSA in D_2O solution, in particular, the thermal dynamics.

EXPERIMENTAL

Crystallized BSA (Lot V73811) was purchased from Reheis Chemical Co. (Phoenix, AZ), and all reagents were purchased

Received 19 March 2007; accepted 8 June 2007.
* Author to whom correspondence should be sent. E-mail: yyylaw@263.net.

0003-7028/07/6109-0921$2.00/0

from Sigma (St. Louis, MO). Distilled deionized water was used throughout for the purification procedure. BSA was purified through the procedure proposed by Chen and modified by Sogami and Foster.[57] Dimer and higher aggregates were removed by the gel-filtration technique with TOYOPEARL HW-55F (Tosoh Corp. Tokyo, Japan).

Prior to infrared experiments, purified BSA was dissolved in D_2O at 25 °C for two days. The protein sample was lyophilized from D_2O. This procedure was performed twice for each sample. For measurement, the sample lyophilized was dissolved in D_2O containing 0.1 M sodium chloride. Sample pD was measured with a standard pH electrode and the value was corrected according to pD = pH + 0.4 for deuterium isotope effects. The protein concentration was determined by assuming a molar extinction coefficient at 280 nm of 6.67. The final concentration of defatted BSA solution in D_2O was 2.0 wt % with an ionic strength of 0.1 M, and the pD value of the sample was 5.40.

Infrared spectra were recorded on a Nicolet Magna 760 spectrometer equipped with a liquid nitrogen cooled mercury cadmium telluride (MCT) detector and continuously purged with dry air. BSA solution was placed between a pair of CaF_2 windows separated with a 50 μm Teflon spacer, and then in a thermostated cell. For each temperature, 256 interferograms were coadded and Fourier transformed employing a Happ–Genzel apodization function to generate a spectrum with a nominal resolution of 2 cm^{-1}. The sample temperature was controlled by means of a circulation water system. To obtain spectra at discrete temperatures, the protein solutions were heated at an interval of 2 °C over the temperature range of 26–90 °C. Spectra at these temperatures were recorded by equilibrating the sample for 5 min prior to data collection. IR spectra of buffer solution were recorded under identical conditions.

OMNIC (Nicolet Co.) and Grams (Galactic Co.) software were employed for data acquisition and pretreatment of IR spectra, respectively. Contributions of D_2O to the spectrum of a protein solution were eliminated by subtracting spectra of D_2O at the same temperature as that of BSA solution, in such way that the baseline was flat between 2000 and 1800 cm^{-1}. Minor spectral contributions from residual water vapor were eliminated using a set of water vapor spectra, as described by Fabian et al.[58,59] Fourier self-deconvolution (FSD)[60] was carried out to resolve the overlapping of IR bands using a half-bandwidth of 19.8 cm^{-1} and a band-narrowing factor $k = 1.8$. The final protein spectra were used for further analysis. EFA was carried out for the final protein spectra to calculate spectral and kinetic profiles by using a Matlab (Eigenvector Research Inc., MA) program, which was compiled by one of the authors (B. Yuan).

DATA TREATMENT

The temperature-dependent difference IR spectra of defatted BSA in D_2O are organized in a data matrix **D**, the rows of which are the difference spectra at each temperature and the columns of which represent the kinetic profiles (absorbance versus temperature) at each wavenumber.

Evolving factor analysis decomposes the data set **D** into the product of two small matrices **X** and $\mathbf{Y}^T$, as shown in Eq. 1:

$$\mathbf{D} = \mathbf{x}_1\mathbf{y}_1^T + \mathbf{x}_2\mathbf{y}_2^T + \cdots + \mathbf{x}_N\mathbf{y}_N^T = \mathbf{X}\mathbf{Y}^T + \mathbf{E} \qquad (1)$$

N is the number of selected factors determined by singular value decomposition (SVD) of **D**. Matrix **X** contains N pure column kinetic profiles, and matrix $\mathbf{Y}^T$ contains N pure row spectral profiles. Matrix **E** describes the experimental error, that is, the residual variation of the data set that is attributed to noise.

The algorithm of EFA begins by first estimating **X** (the kinetic profiles) using a series of SVDs with both a forward and a backward version of data set **D**. That is, the singular values of the factors in the forward and backward sequences are joined at the points at which they cross in the forward and backward directions, and these curves constitute the first rough estimation of **X**. Then, the matrices **X** and $\mathbf{Y}^T$ are calculated iteratively by estimating $\mathbf{Y}^T$ and **X** alternately while applying the appropriate constraints. Typical constraints are non-negativity of kinetic (**X**) and spectral ($\mathbf{Y}^T$) profiles and unimodality of kinetic (**X**) profiles. In this application, only the non-negativities of **X** and $\mathbf{Y}^T$ were assumed. The iterative procedure was terminated when the normalized correlation coefficient between successive iterations of **X** and $\mathbf{Y}^T$ were both greater than 1×10^{-9}. A more detailed description of the above procedure can be found in Ref. 37.

Commonly, the sum of the concentrations of the N factors should be a constant in the evolutionary process:

$$\sum_{n=1}^{N} x_{in} = \text{constant} = 1 \qquad (2)$$

where x_{in} is the intensity of factor n at the temperature i. So it may be better to correct **X** according to Eq. 2. First, a set of parameters for correction was calculated by

$$\mathbf{c} = \mathbf{X}^+\mathbf{I} \qquad (3)$$

where **c** is a column vector of $[\mathbf{c}_1\ \mathbf{c}_2\ \cdots\ \mathbf{c}_N]$, **I** is a column vector of ones, and $\mathbf{X}^+$ is the pseudoinverse of **X**. Then the kinetic profiles were corrected by multiplying the respective parameter,

$$\mathbf{X}_{corr} = \mathbf{X}\,\mathbf{diag}(\mathbf{c}) \qquad (4)$$

where **diag(c)** is an $N \times N$ matrix whose diagonals are c_1, c_2, ..., c_N. Finally, the spectral profile ($\mathbf{Y}^T$) was accordingly corrected by using $\mathbf{X}_{corr}$ on the basis of Eq. 1.

In the figures presented below, the columns of **X** are taken as the resolved temperature profiles of each species, while the rows of $\mathbf{Y}^T$ are taken as the resolved spectral profiles of the species.

RESULTS AND DISCUSSION

Heat-Induced Denaturation of Defatted Bovine Serum Albumin in D_2O Solution Monitored by Infrared Spectra. Figure 1 shows temperature-dependent (26–90 °C) difference spectra in the 1700–1600 cm^{-1} region of defatted BSA in D_2O solution calculated by subtracting the corresponding spectrum of D_2O from the original IR spectrum at the same temperature. The difference spectra were used for further analysis in the following sections. In the process of temperature elevation, the intensity of the band near 1654 cm^{-1} decreases while the intensities of the bands near 1682 cm^{-1} and 1616 cm^{-1} increase. It is noted that the position of the band near 1654 cm^{-1} seems to shift to lower wavenumber with the rise of temperature. But actually, a new band develops near 1644

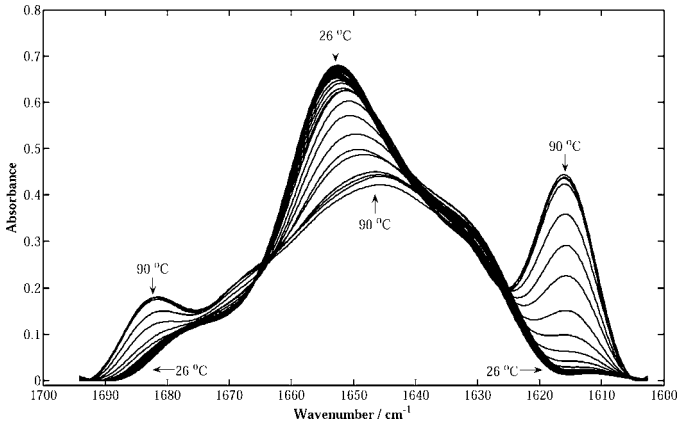

FIG. 1. Difference IR spectra of defatted BSA in D_2O solution (2.0 % wt) in the temperature range of 26–90 °C, by subtracting the contribution of D_2O at the same temperature in the spectral region of 1700–1600 cm^{-1}.

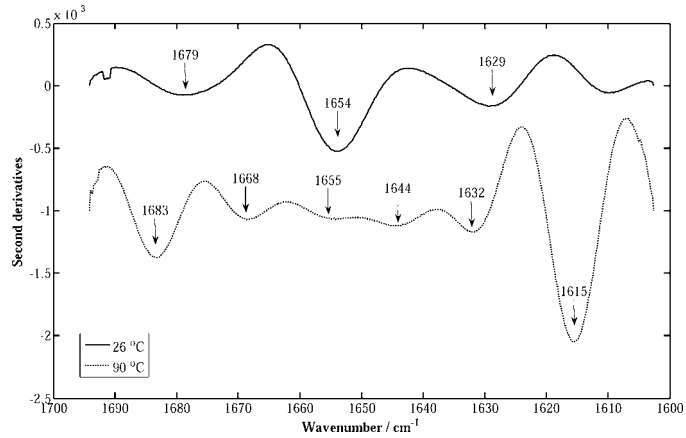

FIG. 2. Corresponding second derivatives of the difference IR spectra in Fig. 1 at 26 °C and 90 °C, respectively.

cm^{-1} at high temperature, which is proved in the following discussion.

Second-Derivative Spectra. Figure 2 plots the corresponding second derivatives of the difference spectra in Fig. 1 at 26 °C and 90 °C, respectively. The second derivative at 26 °C yields downward peaks at 1679 cm^{-1}, 1654 cm^{-1}, and 1629 cm^{-1}, which are assigned to the β-turns, α-helices, and short-segment chains connecting with the α-helical segments, respectively.[16,20–22] The assignment of the band near 1630 cm^{-1} is controversial, but we do not agree with it's assignment to the intra-molecular β-sheet, just as for many proteins, which has been discussed in our previous work.[16] The second derivative at 90 °C yields downward peaks at 1683 cm^{-1}, 1668 cm^{-1}, 1655 cm^{-1}, 1644 cm^{-1}, 1632 cm^{-1}, and 1615 cm^{-1}. It is noted that there exist two bands near 1650 cm^{-1}, the bands at 1655 cm^{-1} and 1644 cm^{-1}, which are assigned to the α-helices and random coils, respectively. Therefore, it can be concluded that temperature rise does not cause the band near 1654 cm^{-1} to shift to lower wavenumber as seen from Fig. 1 but causes a new band due to random coils developed at 1644 cm^{-1}, indicating the loss or collapse of secondary structures.[7] In fact, the random coil formations exist only when the temperature is high enough to cause the protein denaturation. At 90 °C, two new bands can be identified at 1683 cm^{-1} and 1615 cm^{-1}, respectively, which are both associated with the intermolecular β-sheets.[16] More exactly, the band at 1683 cm^{-1} is assigned to the anti-parallel β-sheets while the other band at 1615 cm^{-1} arises from the intermolecular β-sheets resulting from the aggregation.[16] Because the native BSA is revealed by the absence of the β-sheet structure from the X-ray crystallographic study of HAS,[50] the formation of the β-sheet indicates the heat-induced distortion of the secondary structure of BSA. Additionally, compared with the corresponding bands at 26 °C, the band at 1632 cm^{-1} due to short-segment chains connecting with the α-helical segments slightly shifts to higher wavenumber, while the band at 1668 cm^{-1} due to the β-turns shifts to lower wavenumber. The assignments of the bands observed in the difference IR spectra and the corresponding second derivatives are summarized in Table I.

It can thus be concluded from the second derivatives of the temperature-dependent IR spectra of defatted BSA in D_2O solution that the content of α-helices decreases, while the content of random coils and β-sheets increases in the process of temperature elevation. But the kinetics of heat-induced secondary structural changes of defatted BSA in D_2O remain unknown.

Kinetics Obtained from Conventional Spectral Analysis Methods. The absorbance of the bands associated with secondary structural components of protein are usually used to monitor the changes caused by environmental factors, such as pH, temperature, pressure, and so on. Here, the heat-induced variations of the absorbance of the bands at 1615 cm^{-1}, 1630 cm^{-1}, 1654 cm^{-1}, and 1670 cm^{-1} in Fig. 1, which are due to the intermolecular β-sheets, short-segment chains connecting the α-helical segments, α-helices, and β-turns, respectively, are plotted in Fig. 3. The intensity profiles of the bands at 1615 cm^{-1} and 1674 cm^{-1} indicate that the remarkable increase of β structures (β-sheets and β-turns) occurs in the temperature range of 68–82 °C, while the intensity profile of the band at 1654 cm^{-1} indicates that the loss of α-helices successively undergoes a slight and a rapid transition, which approximately occur in the temperature ranges of 56–68 °C and 68–82 °C, respectively. Usually, the intensity change of a shoulder band cannot provide the exact kinetic profile. So we cannot confirm the temperature-dependent variation of the short-segment chains connecting the α-helical segments from Fig. 3. In our previous study,[16] the peak height intensities of individual Gaussian components obtained from the curve fitting using a Gaussian line shape were employed to investigate the heat-induced changes of the secondary structures of BSA. The results demonstrate that the transition temperature of the α-helices, turns, and intermolecular β-sheets of BSA is around 75 °C, while the transition temperature of short-segment chains connecting the α-helical segments is only 61.1 °C, which indicates that the variation of secondary structures of BSA undergoes a multi-transition procedure with the temperature rise.

On the basis of our previous study,[16] the curve-fitting method was used to estimate the contents of the secondary structures of BSA in the process of temperature elevation in the present study. The spectra were fitted with a Gaussian line shape by taking the number of bands and their positions from the second derivatives. The correlation coefficient between the original spectrum and the fitted spectrum is above 0.999. The contents are estimated by the ratios of the areas of individual Gaussian profiles associated with the corresponding secondary structures of BSA to the sum area. Figure 4 shows the

TABLE I. Frequencies (cm^{-1}) and assignments of IR bands of defatted BSA in D_2O solution observed in the second-derivative IR spectra at 26 °C and 90 °C, and the spectral profiles from two-factor EFA and three-factor EFA.

Second derivative		Two-factor EFA		Three-factor EFA			
26 °C	90 °C	1st factor	2nd factor	1st factor	2nd factor	3rd factor	Assignment
	1683		1682			1682	Anti-parallel β-sheet
1679	1668	1679	1669	1679	1677	1669	β-turn
1654	1655	1652	1653	1652	1650	1653	α-helix
	1644		1645			1645	Random coil
1629	1632	1629	1632	1629	1629	1632	Short-segment chains connecting α-helical segment
	1615		1616		1614	1616	Intermolecular β-sheet

temperature-dependent changes of the content of intermolecular β-sheets (1615 cm^{-1}), short-segment chains connecting α-helical segments (1630 cm^{-1}), α-helices (1654 cm^{-1}), and β-turns (1670 cm^{-1}), respectively. Intermolecular β-sheets and β-turns rapidly increase in the temperature range of 68–82 °C, while α-helices rapidly decrease in the same temperature range, which indicates that these three secondary structures are cooperatively denatured on heating. On the other hand, a small part of the short-segment chains connecting the α-helical segments is gradually lost in the temperature range of 56–74 °C and the slight decrease of α-helices starts at the temperature of 56 °C.

Thus, the above results indicate that heat-induced denaturation of BSA in D_2O is a multi-transition process. Short-segment chains connecting α-helical segments and α-helices are slightly lost from 56 °C, while the rapid increases of intermolecular β-sheets and β-turns cooperatively occur with the rapid decrease of α-helices in the temperature range of 68–82 °C.

Evolving Factor Analysis: Determination of the Number of Factors. The number of selected factors employed in EFA can be determined by SVD. Figure 5 plots the results obtained for the SVD of the experimental data set, in which singular values are presented as a function of the number of factors. The first two factors obviously have significant contributions to spectral variations. But it is a little difficult to decide whether the third factor arises from noise or not. From the SVD plots in Fig. 5, the singular value of the third factor is above noise level. However, the percentages of the variance captured in the first, second, and third factors are 96.73%, 3.23%, and 0.03%, respectively, that is, the singular value associated with the third factor is insignificant compared to those values associated with the first two factors. So it may be feasible to select two or three factors in EFA of the difference IR spectra of defatted BSA in D_2O. Then the results from two-factor EFA and three-factor EFA should be compared.

Initialized Kinetic Profiles for Evolving Factor Analysis Iteration. Before starting the iteration to estimate the kinetic profiles and spectral profiles, the initialized kinetic profiles should be calculated according to the algorithm described in the data treatment method. Here, the kinetic profile is expressed as temperature profile. Figure 6a displays the plots of the singular values of the first three factors calculated in the forward and backward directions. The solid lines present the forward singular value plots, while the dashed lines present the backward singular value plots. The lines with empty circles, empty squares, and no markers are attributed to the first, second, and third factors, respectively. The singular value of the third factor from Fig. 6a seems to be over the noise level. Thus, it may be better to explain all of the spectral variations by selecting three factors in EFA, which are discussed in further detail in the following section. On the basis of the forward and backward singular value plots, the initialized temperature profiles for two-factor EFA and three-factor EFA were calculated and presented in Fig. 6b and Fig. 6c, respectively.

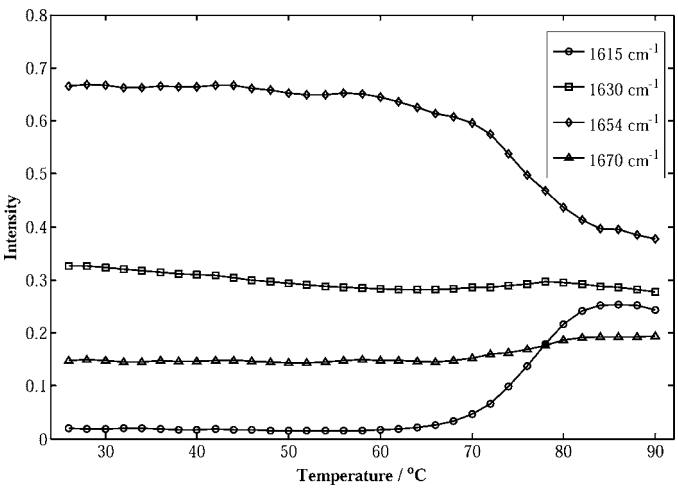

FIG. 3. Plots of the absorbance of the spectra in Fig. 1 as a function of temperature at 1615 cm^{-1}, 1630 cm^{-1}, 1654 cm^{-1}, and 1670 cm^{-1}, respectively.

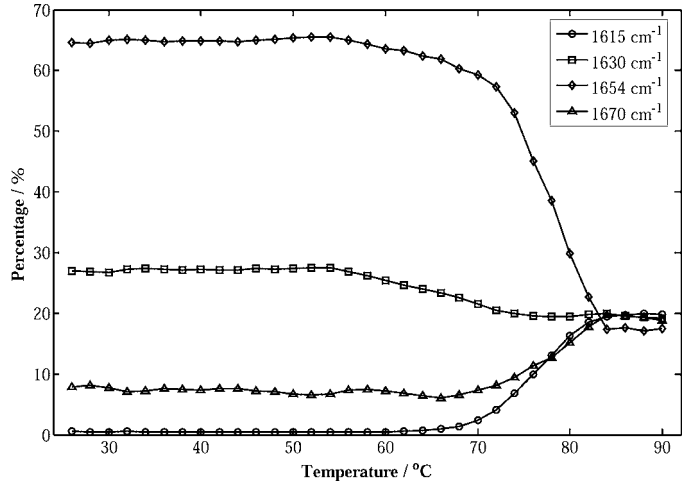

FIG. 4. Temperature-dependent variations of the contents of secondary structural components associated with intermolecular β-sheets (1615 cm^{-1}), short-segment chains connecting α-helical segments (1630 cm^{-1}), α-helices (1654 cm^{-1}), and β-turns (1670 cm^{-1}) of BSA, respectively.

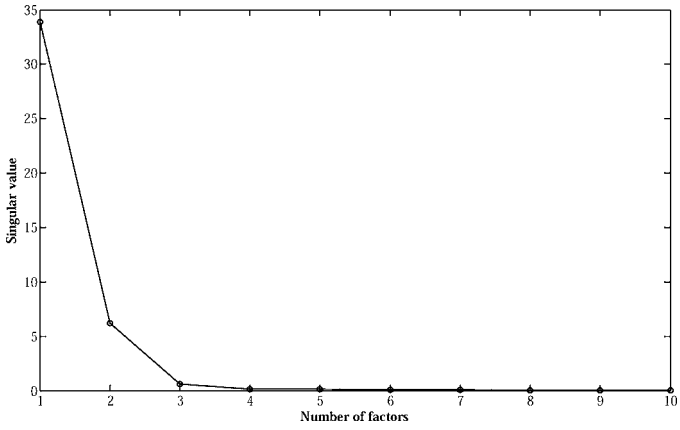

FIG. 5. SVD of the temperature-dependent spectral data.

Two-Factor Evolving Factor Analysis. The spectral and temperature profiles calculated from two-factor EFA are shown in Fig. 7. The solid line and dashed line in Fig. 7a present the spectral profiles of the first and second factors, respectively, and the lines with empty circles and empty squares present the temperature profiles of the first and second factors, respectively. In the spectral profile of the first factor, three peaks due to β-turns, α-helices, and short-segment chains connecting with α-helical segments are observed at 1679 cm^{-1}, 1652 cm^{-1}, and 1629 cm^{-1}, respectively. The spectral profile of the first factor is similar to the spectral feature at 26 °C, which indicates that the first factor is associated with the native protein. The spectral profile of the second factor displays six peaks at 1682 cm^{-1}, 1669 cm^{-1}, 1653 cm^{-1}, 1645 cm^{-1}, 1632 cm^{-1}, and 1616 cm^{-1}, respectively. The bands at 1669 cm^{-1}, 1653 cm^{-1}, and 1632 cm^{-1} are due to β-turns, α-helices, and short-segment chains connecting with α-helical segments, respectively.[16,20–22] However, the band at 1645 cm^{-1} is assigned to random coils and two sharp peaks at 1682 cm^{-1} and 1616 cm^{-1} both arise from intermolecular β-sheets.[16,20–22] Random coils and intermolecular β-sheets are the secondary structures of BSA mostly existing in its denatured state. So the second factor is associated with the denatured protein. The assignments of the bands in the spectral profiles are also summarized in Table I. The temperature profiles obtained from two-factor EFA indicate that the protein in D_2O undergoes a transition from native state to denatured state with temperature rise and the cross temperature of transition is 76 °C, at which the concentrations of native and denatured protein in solution is equal. Moreover, it can be observed from the temperature profiles that the remarkable decrease in the content of native protein and the remarkable increases in the content of denatured protein both occur in the temperature range of 68–82 °C. So the results obtained from two-factor EFA indicate that heat-induced conformational changes of the protein in D_2O is only a two-state (native state and denatured state) transition.

Three-Factor Evolving Factor Analysis. Figure 8 shows the spectral and temperature profiles obtained from three-factor EFA. The solid line, dotted line, and dashed line in Fig. 8a represent the spectral profiles of the first, second, and third factors, respectively, and the lines with empty circles, empty triangles, and empty squares in Fig. 8b represent the temperature profiles of the first, second, and third factors, respectively. The spectral profiles of the first and third factors are close to those of the first and second factors obtained in the two-factor EFA, which indicates that the first and third factors are associated with the native and denatured protein, respectively. In the spectral profile of the second factor, four peaks due to β-turns, α-helices, short-segment chains connecting with α-helical segments, and intermolecular β-sheets are observed at 1677 cm^{-1}, 1650 cm^{-1}, 1629 cm^{-1}, and 1614 cm^{-1}, respectively.[16,20–22] Comparing with the spectral profile of the first factor, the intensity of the band near 1652 cm^{-1} slightly decreases and a new band develops near 1614 cm^{-1},

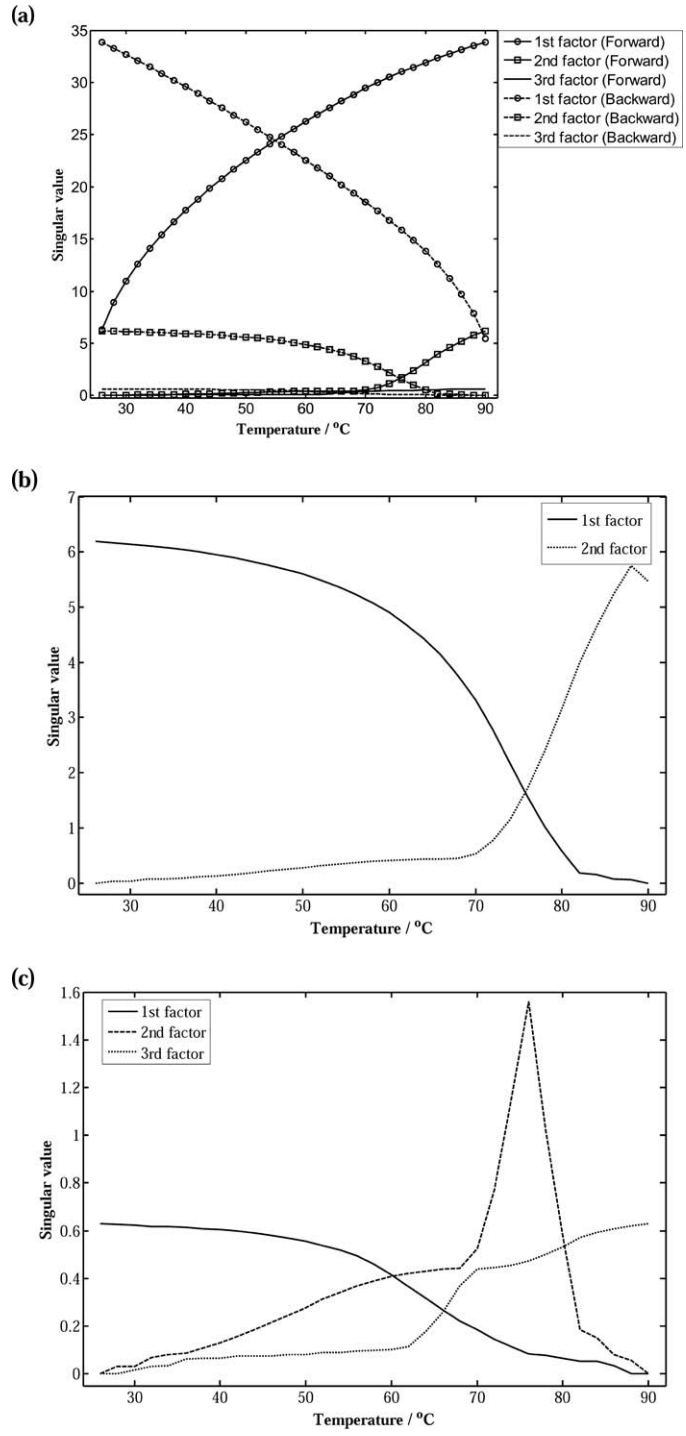

FIG. 6. (**a**) Forward and backward singular value plots of the first three factors calculated by a series of SVDs. (**b**) The initialized temperature profiles for two-factor EFA. (**c**) The initialized temperature profiles for three-factor EFA.

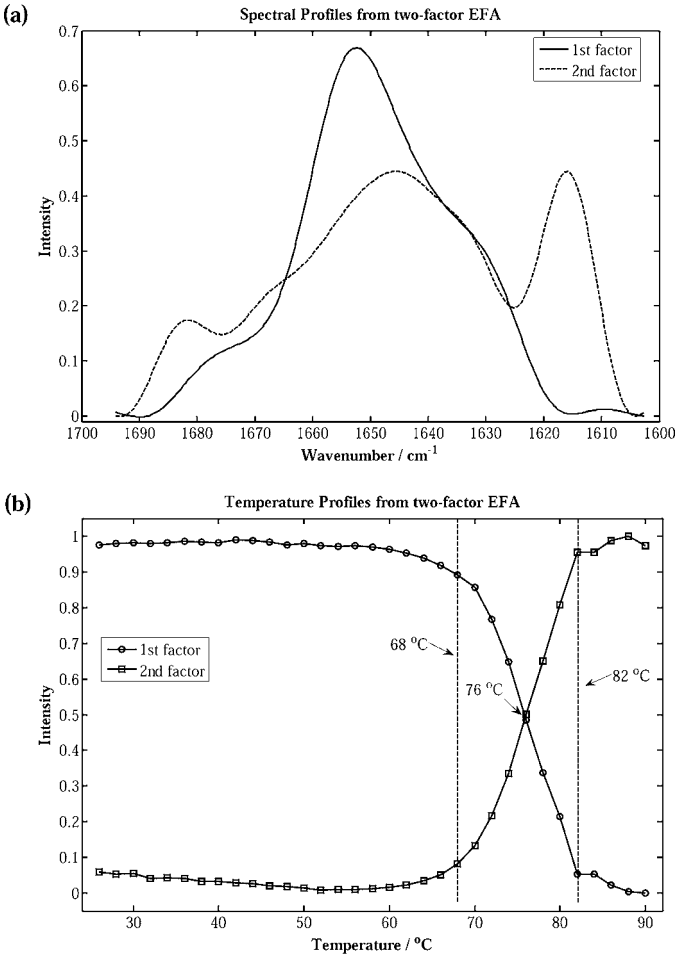

FIG. 7. (**a**) Spectral profiles and (**b**) temperature profiles obtained from two-factor EFA.

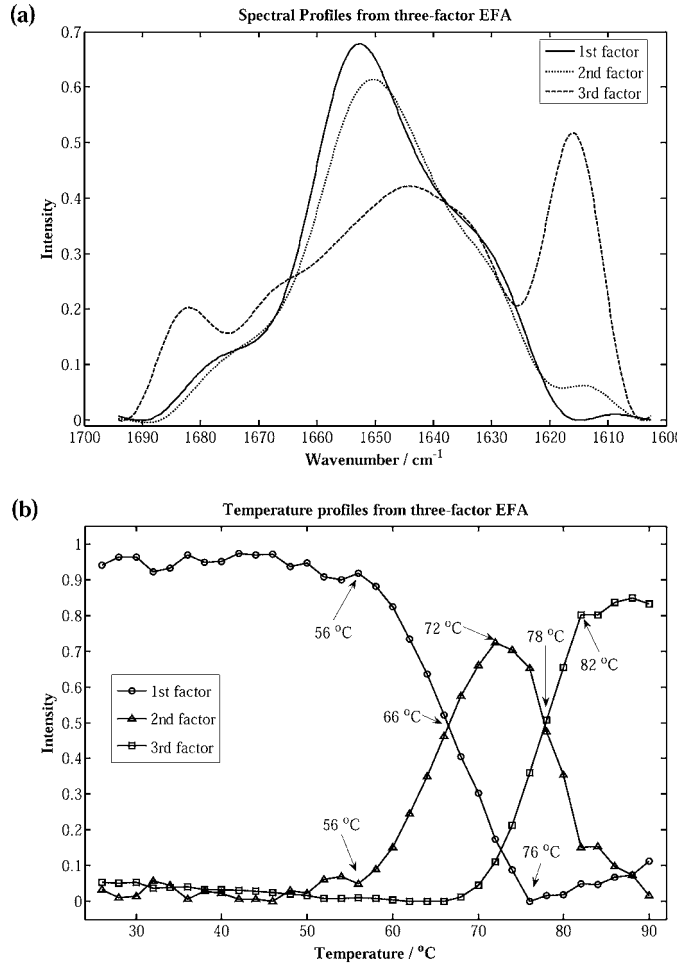

FIG. 8. (**a**) Spectral profiles and (**b**) temperature profiles obtained from three-factor EFA.

indicating the loss of α-helices and formation of β-sheets. So the second factor is associated with the protein species with intermolecular β-sheet conformation and without random coil conformation, which is different from the native and denatured protein. Here, we defined the protein species as a transitional protein. The temperature profiles obtained from three-factor EFA indicate that the protein in D_2O undergoes two two-state transitions and the cross temperature of the first transition from native protein to transitional protein is 66 °C and that of the second transition from transitional protein to denatured protein is 78 °C. The content variations of the three protein species do not occur simultaneously. The content of native protein decreases significantly in the temperature range of 56–76 °C, the content of denatured protein increases significantly in the temperature range of 68–82 °C, and the content of transitional protein first increases from 56 °C and then decreases from 72 °C. In other words, in the process of temperature elevation only the first transition exists before 68 °C and only the second transition exists after 76 °C, while both of the transitions exist in the temperature range of 68–76 °C. By comparing the spectral profiles of the three factors, the first transition from native protein to transitional protein is a slight conformational variation, while the second transition from transitional protein to denatured protein is a drastic conformational variation. The latter is similar to the transition obtained from two-factor EFA. The results obtained from three-factor EFA indicate that the heat-induced denaturation of BSA D_2O is a two-transition process, which is in accordance with the kinetics obtained by conventional spectral analysis methods. Therefore, three-factor EFA provides insight into not only the remarkable conformational variation at higher temperature but also the slight conformational variation at lower temperature for the protein in D_2O in the process of temperature elevation, which makes it a more useful tool to investigate the thermal dynamics of protein in D_2O.

CONCLUSION

In the present study, second-derivative spectra, two-factor EFA, and three-factor EFA have been successfully used to analyze the temperature-dependent IR spectra of defatted BSA in D_2O. In particular, the present study has demonstrated the potential of EFA to effectively monitor the heat-induced unfolding process of protein in D_2O.

The results obtained from two-factor EFA and three-factor EFA have been compared and we have found that three-factor EFA is more effective to investigate the thermal dynamics of protein in D_2O because it can detect not only drastic variation but also slight variation in the secondary structure of protein in D_2O in the process of temperature elevation. The results obtained from three-factor EFA indicate that drastic variation and slight variation occur in the temperature range of 68–82 °C

and 56–76 °C, respectively. The present study has also revealed that the protein in D_2O undergoes two two-state transitions with temperature rise.

ACKNOWLEDGMENT

The authors would like to thank Prof. Y. Ozaki (Kwansei-Gakuin University, Japan) for the helpful discussion.

1. R. J. H. Clark and R. E. Hester, Eds., *Biomolecular Spectroscopy* (John Wiley and Sons, Chichester, 1993), vol. 20, part A, and vol. 21, part B.
2. H. A. Havel, *Spectroscopic Methods for Determining Protein Structure in Solution* (John Wiley and Sons, Chichester, 1995).
3. M. Jackson and H. H. Mantsch, Crit. Rev. Biochem. Mol. Biol. **20,** 95 (1995).
4. H. H. Mantsch and D. Chapman, Eds., *Infrared Spectroscopy of Biomolecules* (John Wiley and Sons, New York, 1996).
5. M. Jackson, M. G. Sowa, and H. H. Mantsch, Biophys. Chem. **68(1–3),** 109 (1997).
6. J. L. R. Arrondo and F. M. Goni, Prog. Biophys. Mol. Biol. **72,** 367 (1999).
7. D. M. Byler and H. Susi, Biopolymers **25,** 469 (1986).
8. A. Dong, P. Huang, and W. S. Caughey, Biochemistry **29,** 3303 (1990).
9. F. Dousseau and M. Pézolet, Biochemistry **29,** 8771 (1990).
10. F. N. Fu, D. B. DeOliveira, W. R. Trumble, H. K. Sarkar, and B. R. Singh, Appl. Spectrosc. **48,** 1432 (1994).
11. W. I. Sungsool, P. Petr, and A. K. Timothy, Biospectroscopy **4,** 93 (1998).
12. E. S. Manas, Z. Getahun, W. W. Wright, W. F. DeGrado, and J. M. Vanderkooi, J. Am. Chem. Soc. **122,** 9883 (2000).
13. M. Weert, P. I. Haris, W. E. Hennink, and D. J. A. Crommelin, Anal. Biochem. **297,** 160 (2001).
14. K. A. Oberg, J. M. Ruysschaert, and E. Goormaghtigh, Eur. J. Biochem. **271,** 2937 (2004).
15. V. Militello, C. Casarino, A. Emanuele, A. Giostra, F. Pullara, and M. Leone, Biophys. Chem. **107,** 175 (2004).
16. K. Murayama and M. Tomida, Biochemistry **43,** 11526 (2004).
17. I. Noda and Y. Ozaki, Appl. Spectrosc. **54,** 236A (2000).
18. Y. M. Jung, B. Czarnik-Matusewicz, and Y. Ozaki, J. Phys. Chem. B **104,** 7812 (2000).
19. C. P. Schultz, O. Bârzu, and H. H. Mantsch, Appl. Spectrosc. **54,** 931 (2000).
20. K. Murayama, Y. Wu, B. Czarnik-Matusewicz, and Y. Ozaki, J. Phys. Chem. B **105,** 4763 (2001).
21. Y. Q. Wu and Y. Ozaki, J. Infrared Milim. Waves **22,** 161 (2003).
22. Y. Ozaki, K. Murayama, Y. Wu, and B. Czarnik-Matusewicz, Spectroscopy **17,** 79 (2003).
23. B. Yuan, H. Y. Zhao, M. Z. Huang, and X. M. Dou, J. Infrared Milim. Waves **23,** 213 (2004).
24. X. Dou, B. Yuan, H. Zhao, G. Yin, and Y. Ozaki, Sci. China, Ser. B **47,** 257 (2004).
25. J. Zhang, H. W. He, Q. Wang, and Y. B. Yan, Protein Peptide Lett. **13,** 33 (2006).
26. Y. J. Kim and G. Yoon, Appl. Spectrosc. **56,** 625 (2002).
27. A. De Juan and R. Tauler, Anal. Chim. Acta **500,** 195 (2003).
28. T. Ishiguro, T. Ono, K. Nakasato, C. Tsukamoto, and S. Shimada, Biosci. Biotechnol. Biochem. **67,** 752 (2003).
29. Y. Etzion, R. Linker, U. Cogan, and I. Shmulevich, J. Dairy Sci. **87,** 2779 (2004).
30. H. S. Lam, A. Proctor, J. Nyalala, M. D. Morris, and W. G. Smith, Lipids **39,** 687 (2004).
31. S. Navea, R. Tauler, E. Goormaghtigh, and A. de Juan, Proteins **63,** 527 (2006).
32. J. Moros, F. A. Inon, M. Khanmohammadi, and A. de Juan, Anal. Bioanal. Chem. **385,** 708 (2006).
33. H. Gampp, M. Maeder, C. J. Meyer, and A. D. Zuberbuler, Talanta **32,** 1133 (1985).
34. M. Maeder, Anal. Chem. **59,** 527 (1987).
35. R. Tauler and E. Casassas, J. Chemom. **3,** 151 (1988).
36. P. Gemperline and J. C. Hamilton, J. Chemom. **3,** 455 (1988).
37. H. R. Keller and D. L. Massart, Chemom. Intell. Lab. Syst. **12,** 209 (1992).
38. A. A. S. C. Machado and J. C. G. E. da Silva, Chemom. Intell. Lab. Syst. **17,** 249 (1992).
39. C. S. P. C. O. Silva, J. C. G. E. da Silva, and A. A. S. C. Machado, Appl. Spectrosc. **48,** 363 (1994).
40. J. C. G. E. da Silva and A. A. S. C. Machado, Chemom. Intell. Lab. Syst. **27,** 115 (1995).
41. W. C. Bell, K. S. Booksh, and M. L. Myrick, Anal. Chem. **70,** 332 (1998).
42. K. Lizuka and T. Aishima, J. Food Sci. **64,** 973 (1999).
43. M. A. Nicholoson, J. F. Aust, K. S. Booksh, W. C. Bell, and M. L. Myrick, Vib. Spectrosc. **24,** 157 (2000).
44. B. Yuan, K. Murayama, Y. Q. Wu, R. Tsenkova, X. M. Dou, S. Era, and Y. Ozaki, Appl. Spectrosc. **57,** 1223 (2003).
45. S. Navea, A. de Juan, and R. Tauler, Anal. Chem. **75,** 5592 (2003).
46. C. Ruckebusch, L. Duponchel, J. P. Huvenne, and J. Saurina, Vib. Spectrosc. **35,** 21 (2004).
47. E. R. Malinowaski and D. G. Howary, *Factor Analysis in Chemistry* (Wiley-Intersicience, New York, 2002), 3rd ed.
48. J. H. Jiang, Y. Liang, and Y. Ozaki, Chemom. Intell. Lab. Syst. **71,** 1 (2004).
49. Z. Zhao and E. R. Malinowski, J. Chemom. **13,** 83 (1999).
50. T. Peters, Jr., *All About Albumin* (Academic Press, New York, 1994).
51. T. Itoh, Y. Wada, and T. Nakanishi, Agric. Biol. Chem. **40,** 1083 (1976).
52. M. Ruegg, U. Moor, and B. Blanc, J. Dairy Res. **44,** 509 (1977).
53. A. Michnik, J. Therm. Anal. Calorim. **71,** 509 (2003).
54. B. J. M. Harmsen and W. J. M. Braam, Int. J. Protein Res. **1,** 255 (1969).
55. V. J. C. Lin and J. L. Koenig, Biopolymers **15,** 203 (1976).
56. A. H. Clark, D. H. P. Saunderson, and A. Suggett, Int. J. Peptide Protein Res. **17,** 353 (1981).
57. M. Sogami and J. F. Foster, Biochemistry **7,** 2172 (1968).
58. H. Fabian, C. Schultz, D. Naumann, O. Landt, U. Hahn, and W. Saenger, J. Mol. Biol. **232,** 967 (1993).
59. H. Fabian, C. Shultz, J. Backmann, U. Hahn, W. Saenger, H. H. Mantsch, and D. Naumann, Biochemistry **33,** 10725 (1994).
60. J. K. Kauppinen, D. J. Mofatt, H. H. Mantsch, and D. G. Cameron, Appl. Spectrosc. **35,** 271 (1981).